Pt(IV)-Based Nanoscale Coordination Polymers: Antitumor Activity, Cellular Uptake and Interactions with Nuclear DNA

N. N. Adarsh[1,+], Carolina Frias[1,+], T. M. Ponnoth Lohidakshan[2], Julia Lorenzo[2], Fernando Novio[1,3], Javier Garcia-Pardo [1,2*] and Daniel Ruiz-Molina[1*]

[1] Catalan Institute of Nanoscience and Nanotechnology (ICN2), CSIC and The Barcelona Institute of Science and Technology, Campus UAB, Bellaterra 08193, Barcelona, Spain.

[2] Institut de Biotecnologia i Biomedicina and Departament de Bioquimica i Biologia Molecular, Universitat Autònoma de Barcelona, 08193 Bellaterra, Barcelona, Spain.

[3] Departament de Química, Universitat Autònoma de Barcelona (UAB), Campus UAB. Cerdanyola del Vallès 08193, Barcelona, Spain

+ Both authors contributed equally to this work

*To whom correspondence should be addressed: Tel.: +34-937373631; Fax: +34-937372648; E-mail: javiergarciapardo@msn.com.

*To whom correspondence should be addressed: Tel.: +34-937373614; Fax: +34-937372648; E-mail: dani.ruiz@icn2.cat.

Abstract

Cisplatin has been for many years the gold standard chemotherapeutic drug for the treatment of a wide range of solid tumors, even though its use is commonly associated with serious side effects including non-selective toxicity, myelosuppression or development of cisplatin resistance, among others complications. Over the last decade, a number of nanoparticle formulations were developed to reduce its side effects and improve the selectivity and efficacy of this drug. In this study, we have developed a novel nanoparticle platform based on nanoscale coordination polymer named (Zn-Pt(IV)-NCPs) which contains a Pt(IV) prodrug , Zn and the linker ligand 1,4-Bis(imidazol-1-ylmethyl)benzene (bix). The main objective has been to gain insights into the mechanism of action of this nanostructured material in comparison with cisplatin and the free Pt(IV) prodrug in order to stablish a correlation between nanostructuration and therapeutic activity. Zn-Pt(IV)-NCPs nanoparticles displayed an average size close to 200 nm as determined by DLS, a good stability in physiologic environments, and a controlled drug release of Pt. *In vitro* studies demonstrated that Pt(IV)-NCPs showed an enhanced cytotoxic effect against cell culture of cervical cancer, neuroblastoma and human adenocarcinoma cells in comparison with free Pt(IV) prodrug. Although no difference in cell uptake of Pt was observed for any of the three cell lines assayed, a higher amount of Pt bound to the DNA was found in the cells treated with the nanostructured Pt(IV) prodrug. These studies suggest that the nanostructuration of the prodrug facilitate its activation and induce a change in the mechanism of action related to an increased interaction with the DNA as corroborated by the studies of direct interaction of the Pt(IV) prodrug, nanostructured or not, with DNA.

Keywords

Nanoscale coordination polymers; cisplatin; nanoparticles; platinum; cisplatin; platinum prodrug

1. Introduction

Cisplatin, also termed as *cis*-diaminedichloroplatinum (II) or CDDP, is one of the most widely known and effective drugs used in chemotherapy [1]. This platinum (II)-based molecule is a coordination complex capable to induce cellular apoptosis due to its ability to form intrastrand crosslinks and other adducts with DNA [2, 3]. After its FDA approval in 1978, it has been used for treatment of a variety of human solid tumors, including bladder, head and neck, non-small cell lung cancer (NSCLC), small cell lung cancer (SCLC), ovarian, testicular cancers and neuroblastoma, among others [3]. Although cisplatin is the first-line treatment for the majority of these cancers, the administration of this drug presents many drawbacks. One of the most important is the lack of tumor tissue selectivity leading to important side effects including nephrotoxicity, ototoxicity and or neurotoxicity [4-6]. Moreover, the administration of high doses over time may cause myelosuppression and acquired drug resistance [7, 8]. To overcome such limitations, a series of new cisplatin analogues have been synthetized, and six of them have gained marketing approval over the last thirty years [9]. However, there are still severe side effects associated with the use of these drugs, which notably limit their administration and clinical effectiveness [9, 10].

During the last decade, a variety of nanostructured systems have been developed as carriers to improve the therapeutic efficacy and decrease the toxicity of cisplatin and cisplatin analogues [11-14]. These systems include organic, inorganic and hybrid nanoparticles. Typically such systems follow two different strategies for drug loading; 1) the direct encapsulation of the drug by physical entrapment; 2) incorporation of the active molecule as building block. Among hybrid nanoparticles, Nanostructured Coordination Polymers (NCPs) present important and unique features, such as its chemical tunability, intrinsic biodegradability and high drug loading capacity. In addition, these nano-platforms have demonstrated promising preclinical results, since exploit what is called the enhanced permeability and retention (EPR) effect [15] and display more controlled and efficient drug release profiles [16, 17]. NCPs are nanoparticles

made from the coordination of a metal ion or metal complex that can be polymerized by using adequate linker ligands [17-19]. In these systems, the therapeutic specie can be encapsulated during the nanoparticles formation or act as building blocks what determines the release rate of the active specie [17]. One of the methodologies used for minimize the side effects of cisplatin derivatives is to use the oxidized form Pt(IV) as inactive prodrug molecule. These Pt(IV) complexes remains inactive in physiological conditions meanwhile in intracellular conditions it can become into the pharmacologically active Pt(II) form by the action of reducing agents (i.e. ascorbic acid (AA) or glutathione) [14]. The transformation of the square-planar Pt(II) species into Pt(IV) octahedral complexes has a valuable benefit since this geometry allow polymerize the Pt(IV) units through the axial positions as previously reported [14]. The first family of Pt(IV)-based NCPs was developed by Lin and coworkers in 2008, by using disuccinatocisplatin (DSCP) as Pt(IV) prodrug. This novel strategy for delivery of Pt-based drugs demonstrated unprecedented chemotherapeutic efficiency towards two different cancer cell lines *in vitro* [16]. In 2103, the same research group reported the synthesis of lipid-coated coordination polymers based on Zr^{4+} or La^{3+} metal ions and the DSCP ligand as main building block, obtaining spherical nanoparticles, with a controlled drug release of cisplatin and with enhanced cytotoxic effects against two small cell lung cancer cell lines [20]. Additionally, when these lipid-coated nanoparticles were functionalized with anisamide, an enhanced uptake of the nanoparticles was further demonstrated by confocal microscopy and binding assays [20]. From these seminal works, a series of lipid coated and pegalyted NCPs derived from zinc phosphate and cisplatin or oxaliplatin Pt(IV) prodrug were tested *in vivo* in mice, in both cases showing superior antitumor activity compared with free drugs [21]. Although the large number of studies that have been performed with Pt(IV)-based NCPs, there is a lack of knowledge concerning the action mechanisms of the Pt(IV) prodrugs and the effect of its nanostructuration. In this scenario, our objective is to bring some light on the therapeutic effect of the Pt(IV) prodrugs nanostructuration.

Hence, in this work, novel Pt(IV) prodrug-based nanostructured coordination polymer particles, termed Zn-Pt(IV)-NCPs, were synthetized and extensively characterized. The stability of the nanoparticles, as well as the Pt release, were studied under physiologic conditions. We have also studied the interaction of the released platinum species with DNA by electrophoretic mobility measurements. Additionally, the Pt uptake and the amount of Pt bound to the DNA in three different tumor cell lines were assessed comparing the nanoparticles with the free Pt(IV) prodrug. The cytotoxicity associated to the nanoparticles was demonstrated on multiple cancer cell lines *in vitro* and compared to the free Pt(IV) prodrug. The results obtained in this study provide important evidences of the influence of the nanostructuration on the biological effectiveness of Pt(IV) prodrugs at cellular level.

2. Materials and Methods

2.1 Materials

All chemical reagents were purchased from Sigma-Aldrich (unless otherwise specified) and used as received. Solvents were obtained from Scharlab and used as received. Cell culture media and culture media supplements were ordered from Life Technologies. 1,4-Bis(imidazol-1-ylmethyl)benzene (bix) was synthesized as previously reported by our group with some modifications (see Supporting Information, A1) [22, 23]. ICP-MS standards and the setup solution were acquired from Perkin Elmer. PrestoBlue™ Cell Viability reagent was purchased from Invitrogen. All the nanoparticles synthetized in the present work were prepared under general aseptic conditions to ensure the suitability of the final material for biological experiments. All the cell lines were obtained from the American Type Culture Collection (ATCC). The DNA was stained with Midori Green (Nippon Genetics).

2.2 Characterization methods

FT-IR spectra were recorded by using a Tensor 27 spectrophotometer (Buker) equipped with a single-reflection diamond window ATR accessory (MKII Golden Gate, Specac). 250 MHz ^{1}H NMR spectra were recorded on a Bruker DPX 250 MHz spectrometer; Powder X-ray diffraction (XRD) pattern was recorded on a X'Pert PRO MRD diffractometer (PANalytical) and X-ray photoelectron spectroscopy (XPS) was performed in a Phoibos 150 analyser from SPECS. A NexION 300X ICP mass spectrometer (PerkinElmer) was used for mass spectrometry measurements. Scanning electron microscopy (SEM) images were captured on a Quanta 650 FEG microscope (FEI) at acceleration voltages of 5–20 kV. Previously, the samples were prepared by drop casting of the corresponding dispersion on aluminum tape followed by evaporation of the solvent under room conditions. All the samples were metalized with a thin layer of platinum (5 nm) by using a Quorum Emitech K550 (Quorum technologies Ltd). Scanning transmission electron microscopy (STEM) images were acquired on a FEI Tecnai F20 transmission electron microscope with a HAADF detector at an applied boltage of 75 kV. Dynamic light scattering (DLS) analysis were performed with a Zetasizer Nano 3600 (Malvern instruments) in a PBS buffer containing 31 mg/ml Bovine Serum Albumin (BSA). Fluorescent images from the nanoparticles were acquired using an Axio-Observer Microscope from Zeiss equipped with a AxioCam HRc camera. A Victor3 fluorescence reader (PerkinElmer's) was used to read the plates in the cytotoxicity assays. A GelDoc XR+ reader from Bio-Rad was used for imaging of agarose gels. An Agilent HP 8453 UV-vis spectrophotometer was used for DNA quantification.

2.3 Synthesis of the Pt(IV) prodrug

The Pt(IV) prodrug was synthetized similarly as previously described [16], with some modifications. Briefly, the Pt(IV) prodrug was prepared through three synthetic steps: 1) The first step starts with the oxidation of cisplatin to oxoplatin, by the addition of hydrogen peroxide

under darkness, with heating and under constant reflux. 2) The resultant product was converted to DSCP by the addition of succinic anhydride, also under darkness, heating and reflux conditions. 3) Finally, DSCP was further converted and stabilized to its bis-propyl ammonium salt. A schematic representation of the synthetic procedure and characterization are shown in Supporting Information, A2.

2.4 Synthesis and characterization of the nanoparticles

Zn-Pt(IV)-NCPs and the nickel analogous Ni-Pt(IV)-NCPs were obtained by a *in situ* fast polymerization reaction of the metal ion (Zn or Ni) with a mixture of two co-ligands: the platinum prodrug salt and bix. The synthesis of Zn-Pt(IV)-NCPs and Ni-Pt(IV)-NCPs were performed following previous procedures reported by our research group [19]. In a typical synthesis Bix (18.2 mg, 0.077 mmol) and Pt(IV) prodrug (50.0 mg, 0.077 mmol) were dissolved in an aqueous ethanol solution (25ml EtOH + 2 ml miliQ H_2O). Under constant stirring at 900 rpm, a solution of $Zn(NO_3)_2$. $6H_2O$ (22.7 mg, 0.077 mmol in 2 mL miliQ H_2O) or $Ni(NO_3)_2$. $6H_2O$ (22.3 mg, 0.077 mmol in 2 mL miliQ H_2O) were added. The rapid coordination of the co-ligands with the metal ions led to the formation of a fine white and pale blue solids of Zn-Pt(IV)-NCPs and Ni-Pt(IV)-NCPs, respectively, that precipitates in few minutes. The reaction was maintained under stirring for 30 min and the resultant precipitates were collected by centrifugation, washed twice with ethanol, and completely dried by lyophilization. A completed and detailed characterization of the obtained nanoparticles has been summarized in Supporting Information, A3.

2.5 Characterization of the Pt Release kinetics

The *in vitro* release kinetics of Pt from the nanoparticles was studied by the dialysis method. Briefly, a dialysis bag (MWCO: 3500 Da, 15 x 5 cm) containing 8 mg of Zn-Pt(IV)-NCPs dispersed in 6 ml sterile PBS (pH 7.4) was placed into 100 ml of PBS solution for 72 hours at 37 ºC and under constant stirring (360 rpm). To determine the release of Pt from the nanoparticles and diffused through the dialysis bag, aliquots of 500 μL of the external solution were taken after different incubation times. Samples were kept at 4 ºC, until the Pt concentration was determined by ICP-MS. Release experiments were performed in triplicate.

2.6 DNA-binding studies.

DNA-Binding experiments were performed using the pBluescript II plasmid as substrate. Reactions containing 2 μg of the DNA plasmid were incubated with different concentrations (0, 1, 10, 100 and 500 μM) of the Pt (IV) prodrug or Zn-Pt(IV)-NCPs for 24 hours at 37 ºC in the absence or presence of ascorbic acid (0.1 μg/μL) in 40 mM Tris-HCL buffer (Ph 7.3) containning 40 mM NaCl. Samples containing the reducing agent ascorbic acid were preincubated for 2 hours before the DNA was added to the samples. Reactions with DNA and different concentrations of cisplatin (0, 0.1, 1, 10 and 50 μM) as control drug were prepared. Afterwards, gel electrophoresis experiments were performed on agarose gels (0.7% agarose in Tri-Acetate-EDTA buffer), by using a Bio-Rad horizontal tank connected variable potential power supply.

2.7 *In vitro* studies

Cell culture. Human BE(2)-M17 (ATCC CRL-2267), HeLa (ATCC CL-2) and MCF-7 (ATCC HTB-22) cell lines were maintained in Opti-MEM™, in Minimum Essential Medium α (MEM-α) medium, or in Dulbecco's Modified Eagle Medium: Nutrient Mixture F-12 (DMEM-F12), respectively. Media were further supplemented with 10 % (v/v) of heat inactivated fetal bovine

serum (FBS) and the cells were grown under a highly humidified atmosphere of 95 % air with 5 % CO_2 at 37 ºC.

Cytotoxicity Experiments. The cytotoxicity of Pt(IV) prodrug and Zn-Pt(IV)-NCPs towards HeLa, BE(2)-M17 and MCF-7 cells was studied by a resazurin-based assay using the PrestoBlue™ Cell Viability Reagent. The cells were seeded in 96-well plates at a concentration of $3.0x10^3$ cells/well in the case of HeLa and at $2.0x10^3$ cells/well in the case of BE(2)-M17 and MCF-7 cells, respectively. After 24 h incubation, cells were then treated with the Pt(IV) prodrug or with the Zn-Pt(IV)-NCPs nanoparticles at different concentrations ranging from 0 to 540 μM (referred to the Pt concentration). After 24 and 72 h treatment, aliquots of μl of the PrestoBlue™ Cell Viability Reagent solution were added to each well and incubated for up to 2 hours at 37 ºC. Fluorescence (γ_{exc}=531 nm and γ_{em}=572 nm) of each well was measured using a fluorescence microplate reader. The cytotoxic effect of the Pt(IV) prodrug and Zn-Pt(IV)-NCPs nanoparticles against the three different cells lines was determined by calculating the half-maximal inhibitory concentration (IC_{50}). Cytotoxicity experiments were performed at least in triplicate.

Cellular uptake of Pt. HeLa, BE(2)-M17 and MCF-7 cells were seeded on 60 mm culture dishes at a cell density of $3.0x10^5$ cells/plate. After 48 h growth, cells were incubated with the Pt(IV) prodrug and Zn-Pt(IV)-NCPs nanoparticles at a concentration of 75 μM (referred to the Pt concentration) for 5 h. Immediately before cell recovery, the plates were washed twice with cold PBS and the cells trypsinized for 10 min at 37 ºC. Afterwards, trypsin was neutralized with 1 volume of fresh medium and aliquots of 10 μl of each cell suspension were collected to count the number of viable cells present in the samples. For Pt quantitation, cell suspensions were transferred to 1.5 ml Eppendorf tubes and the samples centrifuged at 12000 rpm for 5 min. Finally, the supernatants were discarded and the resultant cell pellets were stored at -80 ºC until ICP-MS analysis was performed.

Cellular DNA-bound Pt determination. HeLa, BE(2)-M17 and MCF-7 cells were treated with Pt(IV) prodrug and Zn-Pt(IV)-NCPs nanoparticles similarly as previously described for cellular uptake experiments. Afterwards, cells were washed twice with cold PBS, scrapped, transferred to 1.5 ml Eppendorf tubes and centrifuged at 1200 rpm for 5 min. For DNA extraction, the resultant pellets were resuspended in lysis buffer solution containing 150 mM Tris-HCl (pH 8.0), 100 mM NaCl and 0.5% (w/v) SDS on ice and afterwards centrifuged at 12000 rpm for 15 min and incubated with ribonuclease A (RNase A, 200 μg/mL) for 1 h at 37 ºC. Then, proteinase K (100 μg/mL) was added followed by an incubation of 3 hours at 56 ºC. A volume of phenol/chloroform (1:1) was added, mixed gently, and after a centrifugation step, aqueous phases containing DNA were transferred to sterile tubes. DNA was precipitated with 0.1 volumes of 2 M sodium acetate and 1 volume of absolute ethanol at –20 ºC overnight. DNA samples were washed with 1 ml of 70 % (v/v) ethanol, dried and resuspended in 20 μl of elution buffer (10 mM Tris-Cl, 1 mM EDTA, pH 8.0). The concentration of the isolated DNA was determined by measuring the absorbance at 260 nm using a UV-vis spectrophotometer. Pt-bound to DNA was quantified by ICP-MS.

2.8 Quantification of Pt, Zn and Ni by ICP-MS

To perform ICP-MS determinations, samples were dissolved in concentrated nitric acid (70% HNO_3) at a concentration of 25 mg/ml and incubated at 50 ºC for 18 h under constant sonication. After digestion, samples were diluted with purified water to a final 0.5 % (v/v) HNO_3 solution for chemical formula determination of Pt(IV) prodrug and Zn-Pt(IV)-NCPS nanoparticles, and diluted to a 7 % (v/v) HNO_3 solution to analyze the cells and DNA samples from uptake experiments. Calibration curves of Pt, Zn or Ni were measured from five standard solutions at different concentrations of each metal (from 20 to 200 ppb for compound samples and from 0.5 to 10 ppb for cell and DNA samples), previously prepared by diluting certified

reference metal stock solutions. The concentrations of Pt, Zn or Ni present in the samples were calculated from the corresponding calibration curve, previously adjusted to a linear regression model (R^2>0.99).

3. Results and discussion

3.1 Synthesis and characterization of Zn-Pt(IV)-NCPs

The schematics for the one-pot synthesis of the Zn-Pt(IV)-NCPs is shown in Fig. 1a. The nanoparticles were fabricated by the fast polymerization of $Zn(NO_3)_2$ with a mixture of two linker ligands, the bis-propyl ammonium salt of Pt(IV) prodrug (DSCP) and bix, resulting in the formation of a white precipitate. The Pt(IV) prodrug is used as its propyl ammonium salt form to favor the coordination of the carboxylic group to the metal ions (Zn or Ni). After 30 minutes, the resulting solid material was then collected by centrifugation, washed several times with ethanol, and dried by lyophilization. As shown by scanning electron microscopy (SEM) (Figure 1b-d) Zn-Pt(IV)-NCPs showed spherical morphology and narrow size distribution, whose diameters ranged between 100-200 nm, yielding an average diameter of 148 ± 48 nm. The study of the colloidal stability of the nanoparticles in simulated physiological conditions was further studied by dynamic light scattering (DLS). For this study very stable solution were achieved dispersing 1 mg/ml of Zn-Pt(IV)-NCPs in a phosphate buffered saline (PBS) at pH 7.4 and containing 31 mg/ml of bovine serum albumin (BSA) (Figure 1e). In these conditions, DLS measurements reveal a hydrodynamic diameter of 215 ± 20 nm with an associated polydispersity index (PDI) of 0.238.

X-ray powder diffraction data for different batches showed that the particles are amorphous (Fig. S1). The chemical composition of these particles was first determined by energy-dispersive X-ray spectroscopy (EDX), which confirmed that they contain platinum, chloride, carbon, oxygen, nitrogen and zinc. XPS analysis reveals also the elemental composition and corroborate the presence of Pt(IV) and Zn(II) metal ions (Fig. S2 and S3). The FT-IR of the Zn-

Pt(IV)-NCPs support the presence of bix and the Pt(IV) prodrug coordinated to Zn ions (Fig. S4) as evidenced by the shift of the absorption bands of the carboxylate belonging to the prodrug ligand from 1625 cm^{-1} to 1586 cm^{-1} observed for the Zn-Pt(IV)-NCPs. Additionally, the presence of stretching vibrations attributed to bix at 1520 cm^{-1} and 1076cm^{-1} that appear at 1536 cm^{-1} and 1092 cm^{-1} respectively, indicated the inclusion of the bix ligand into the coordination polymer network.

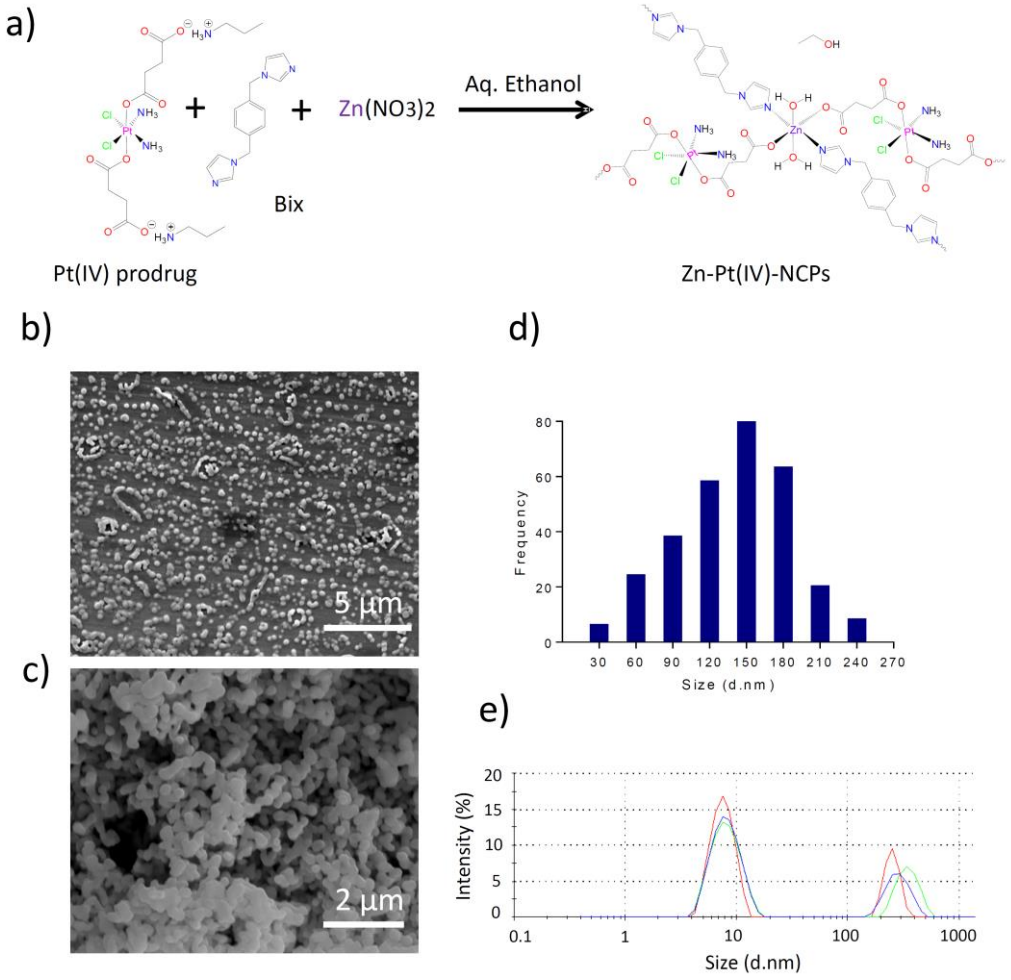

Fig. 1. Synthesis and characterization of Zn-Pt(IV)-NCPs. a) Schematic of Zn-Pt(IV)-NCPs synthesis. b-c) Scanning electron microscopy (SEM) images of Zn-Pt(IV)-NCPs. d) Particle size distribution extracted from SEM images. e) Size distribution of the nanoparticles measured in triplicate by DLS in PBS (pH 7.4) and in the presence of BSA. Note that the peak showed

around 10 nm corresponds to BSA and the one that appears at 200-300 nm is attributed to the nanoparticles.

The elemental analysis of the resulting nanoparticles (Table S1) and ICP-MS results for the measurement of metal contain (See Supporting Information, A3.1) are consistent with the proposed coordination polymer formation with formula $[\{Zn(Bix)(DSCP)(H_2O)_2\}\cdot EtOH]_\infty$ corroborating the presence of one bix ligand, one Pt(IV) prodrug molecule and one Zn metal ion per monomer unit (Fig. S2). Additionally, the chemical formula is completed with one molecule of EtOH and two water molecules, the later presumably in the coordination sphere of Zn ions. In agreement, the nanoscale coordination polymer contains 56.6 ± 0.4 wt.% of the Pt(IV)-prodrug, 7.7 ± 0.5 wt.% of Zn and 26.8 ± 0.6 wt.% of bix. The TGA analysis (Fig. S5) corroborate the presence of the solvent molecules since the thermal decomposition showed a weight loss of 4.72% in the temperature range of 25-150ºC which fits with the loss of 1 molecule of EtOH (calculated weight loss = 5.02%), and another weight loss of 58.51% within the temperature range of 150-900ºC which is attributed to the loss of two water molecules and decomposition of the ligand bix and the co-ligand DSCP (calculated weight loss for 2 molecules of water + 1 molecule of bix + 2 molecule of DSCP = 66.65%). The discrepancy of 8.14% between the calculated and experimental values may be due to the undecomposed fraction of thermally stable DSCP. The remaining weight, close to 35%, would correspond to the non-volatile metal oxides generated after burning completely the sample. Fluorescence microscopy images of the resulting nanoparticles showed an intense blue luminescence (peak centered at approximately 405 nm) when the nanoparticles were excited at 355 nm (Fig. S6). This fluorescence emission is typical for Zn-Bix coordination polymers what demonstrates the coordination of bix with Zn(II) [24] . These optical properties make Zn(bix)-based polymers potential blue fluorescent materials and suggests its possible application for biomedical imaging.

3.2 *In vitro* drug release

When Zn-Pt(IV)-NCPs (1 mg/ml) is dispersed in BSA-containing PBS buffer (31 mg/ml), the nanoparticles present notable stability up to 24 h incubation, indicating that the presence of BSA improves the colloidal stability of the nanoparticles. Under these conditions, the drug release profile of Pt from Zn-Pt(IV)-NCPs was studied for 24 h at 37°C by using dialysis bag method. As shown in Fig. 2, we observed a fast release of the drug during the initial hours, reaching around 50% Pt release at 2 hours and 80% of the total Pt release after 7 hours. Then, a sustainable slow release (~ 10%) takes place during the subsequent 14 hours.

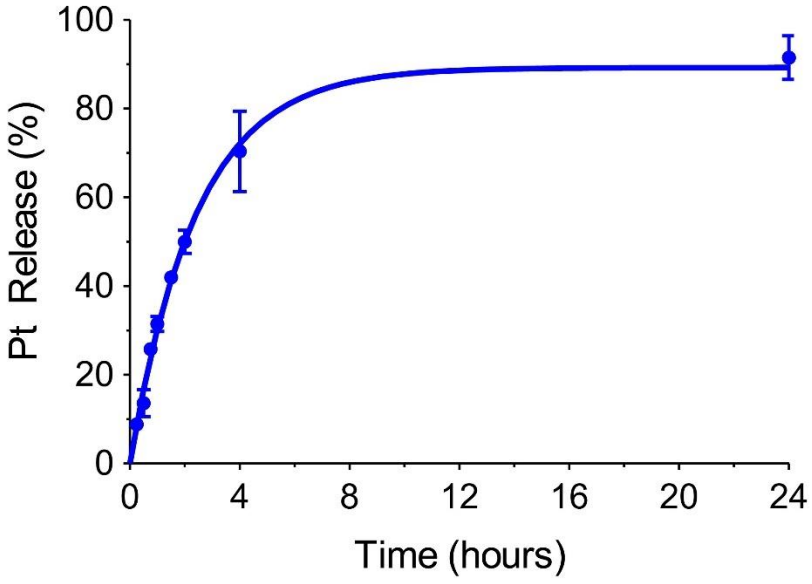

Fig. 2. *In vitro* release kinetics of Pt from Zn-Pt(IV)-NCPs nanoparticles. Experiment was performed in PBS containing 31 mg/ml BSA at pH 7.4 at 37 º in triplicate.

The initial fast release is suggested to be related to the fast degradation of the first layers (soft polymer), meanwhile the more dense core offers an slow release for the remaining material. The overall release fit well with similar systems previously described [16, 17], and give us an information about the chemical stability of the NCPs in solution in physiological conditions. In order to improve their solubility in high-ionic-strength solutions, the nanoparticles were coated with BSA as stabilizer. Serum albumins are attractive natural proteins because they are present

in large amounts in biological fluids (such the human serum), or in fetal bovine serum (FBS), and is commonly used supplement for cell culture media. The use of BSA for stabilizing colloidal dispersions of nanoparticles is a common procedure to increase the stability of different nanoconstructs in physiological media. Alternativeley, other coating materials such as silica, lipids or PEG polymers have been used for stabilize Pt(IV)-based NCPs and increase their colloidal suspensions [16, 25, 26].

3.3 DNA-binding studies

To investigate the effects and interaction of the Pt(IV) prodrug and Zn-Pt(IV)-NCPs nanoparticles on a double- stranded DNA, pBlueScript plasmid was used as the DNA substrate, and the resulting DNA-Pt complexes obtaining after treatment were analyzed by an agarose-gel electrophoresis (Fig. S7). To perform the experiments, different concentrations of the Pt(IV) prodrug or Pt(IV) prodrug-based nanoparticles were incubated for 24 h at 37 ºC in the absence or presence of ascorbic acid. Ascorbic acid (AA) was added to improve the activation of the prodrug through the reduction of Pt(IV) into active Pt(II) as reported previously [27]. In addition, different concentrations of cisplatin were assayed for comparison purposes. The effect of binding of these compounds was determined by their ability to alter the electrophoretic mobility of a plasmid DNA, which presents two majoritarian forms under native conditions: a supercoiled closed circular form (CCC) and an open circular form (OC) [27, 28].

When the Pt(IV) prodrug or Zn-Pt(IV)-NCPs were incubated in the absence of AA, no important effects on DNA migration were observed up to concentrations of 100 μM (Fig. S7). By contrast, the gold standard drug cisplatin caused important effects on the mobility of both the CCC and OC forms of the plasmid DNA at concentrations higher than 10 μM (i.e. 10 and 50 μM) (Fig. S7). In a similar manner, the highest concentration assayed of the Pt(IV) prodrug (i.e. 500 μM) did not caused changes in the mobility of the OC and CCC forms in the absence of AA (Fig. 3). Interestingly, we observed a clear shift of the two OC and CCC bands in the case of the DNA treated with the nanoparticles at the same concentration (see Fig. 3), suggesting a partial activation of the Pt(IV) prodrug from the nanostructured coordination polymer in the

absence of reductant. These bands shift was associated with partial disappearance of the brightness of both OC and CC DNA forms.

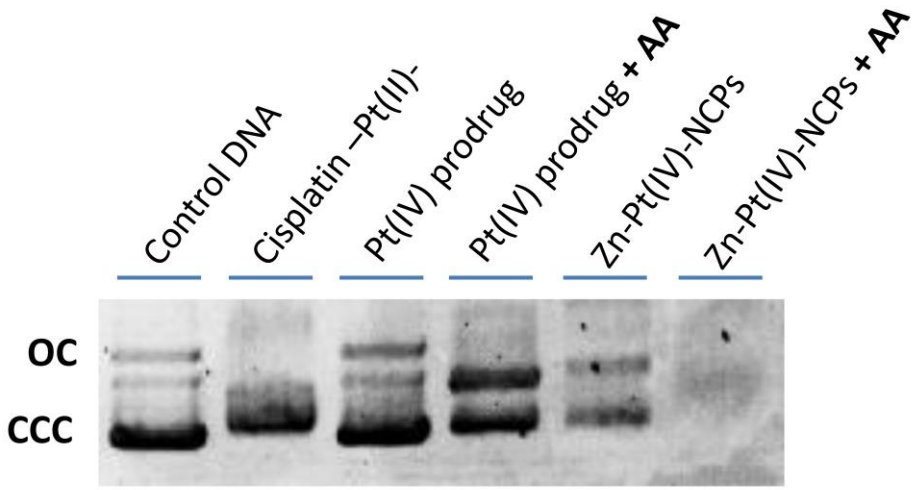

Fig. 3. Agarose gel electrophoresis of a pBluescript II plasmid DNA treated with the Pt(IV) prodrug or Zn-Pt(IV)-NCPs. In both cases the concentration assayed was 500 µM as referred to the Pt concentration and the samples were incubated for 24 h at 37 ºC in 50 mM Tris-HCl (pH 7.3) buffer containing 40 mM NaCl in the absence or presence of 0.1 mg/ml ascorbic acid (+AA). Pure pBluescript II plasmid DNA (Control DNA) and pBluescript II plasmid DNA incubated with 50 µM cisplatin (Cisplatin-Pt(II)-) were prepared as control conditions.

In the presence of ascorbic acid (AA), the Zn-Pt(IV)-NCPs nanoparticles clearly altered the mobility of the plasmid DNA in comparison with the same treatment in the absence of reducing agent (see Fig. 3). Furthermore, we observed an almost complete disappearance of the signal of both OC and CC DNA forms. These results indicate that AA accelerates the conversion of the Pt(IV) prodrug present in the nanostructured coordination polymer to more active Pt (II) species, and points to a redox-dependent mechanism of activation. It is well known that the presence of a reducing environment inside the cells facilitates the intracellular reduction of Pt(IV) prodrugs to active Pt(II) species. This step is thought to be essential for the anticancer

activity of these agents, and involves the loss of the two axial ligands present in the prodrug [14]. Moreover, the use of nanoparticles containing Pt(IV) polymer conjugates is an interesting strategy to preserve the inactive Pt(IV) complex until a reducing environment generates the activate Pt(II) species. Yang et al. demonstrated by electrochemical studies that platinum(IV)-coordinated polymers can more easily lose the axial ligands and be reduced to the corresponding Pt(II) active drug in an acidic environment [29]. In the case of the free Pt(IV) prodrug, incubation with AA clearly altered the mobility of the plasmid DNA compared to the non-treated control or with the DNA treated with the Pt(IV) prodrug alone. As shown in **Fig. 3**, when AA is present in the medium the CCC form runs slightly slower compared to aforementioned conditions, demonstrating a slight progressive unwinding of the supercoiled DNA. This shift in the migration of the CCC form was accompanied by an increase in the mobility of the OC form, which is compatible with the formation of cisplatin 1, 2 intrastrand crosslinks [30]. While the Pt(II) produced upon the activation of the Pt(IV) prodrug are interacting with the DNA, the gel analyses show that they do not form the same complexes induced by the well-known cisplatin (Fig. 3). This phenomenon has been previously demonstrated by other authors for different Pt(IV) prodrugs [27]. In agreement, it has been reported that Pt(IV) complexes can platinate DNA in their oxidized form through the formation of cytotoxic lesions induced by ligand substitution [14].

Taken together, these results from DNA-binding experiments indicate that the Pt(IV) prodrug and the Zn-Pt(IV)-NCPs are interacting with DNA in a concentration-dependent manner. Remarkably, we also show that the Zn-Pt(IV)-NCPs do not require the presence of AA to interact with the DNA, a difference with the non-nanostructured Pt(IV) prodrug. Moreover, partial banishing of the bands associated with the plasmid DNA indicates an interaction of the nanoparticles with the DNA. Such binding might be mediated via electrostatic interactions with the negatively charged phosphate backbone and the electrical charges of the nanostructured coordination polymer. This differential interaction may lead to the aggregation of the DNA limiting the entrance and migration of this Zn-Pt(IV)-NCPs-DNA complexes in the gel.

Considering these results, we suggest a different mode of activation and interaction between the free Pt(IV) prodrug and the nanoparticles with the plasmid DNA.

3.4 *In vitro* Cytotoxicity against cancer cells lines

Human cervical cancer, neuroblastoma, and human adenocarcinoma cells lines (HeLa, BE(2)-M17 and MCF-7, respectively) were used to test the cytotoxicity of the Pt(IV) prodrug and Zn-Pt(IV)-NCPs nanoparticles after 24 h and 72 h treatment. For comparison purposes, cisplatin as control was evaluated under the same experimental conditions. The resultant IC_{50} values are summarized in Table 1.

Table 1. Cytotoxicity of cisplatin, Pt(IV) prodrug and Zn-Pt(IV)-NCPs against three different cancer cells lines.

	Cisplatin (PtII) IC_{50} (nM)[1]	**Pt(IV) prodrug** IC_{50} (μM)[1]		**Zn-Pt(IV)-NCPs** IC_{50} (μM)[1]	
Cell line	24 h	24 h	72 h	24 h	72 h
HeLa	3.5 ± 0.9	>540	431 ± 82	218 ± 21	130 ± 27
MCF-7	2.8 ± 0.4	>540	296 ± 31	249 ± 64	59 ± 8
BE(2)-M17	5.5 ± 0.7	>540	494 ± 66	218 ± 21	133 ± 8

[1] Cell viability in the presence of the indicated compound and referred to Pt concentration.

After 24 h treatment, the Pt(IV) prodrug did not exhibited cytotoxicity against HeLa, MCF-7 or BE(2)-M17 cells, with IC_{50} values higher than 540 μM. By contrast, the Zn-Pt(IV)-NCPs displayed a slight enhanced antitumoral efficacy against the three cell lines, with IC_{50} values below 300 μM. This effect was much evident at longer incubation times. Thus, after 48 h incubation, the IC_{50} values for the Zn-Pt(IV)-NCPs nanoparticles against HeLa, MCF-7 or BE(2)-M17 cells were 1.7-fold, 4.2-fold and 1.6-fold lower than the Pt(IV) prodrug, respectively. This indicates that nanostructuration of a drug increases its cytotoxic effect, and suggests that maintaining the therapeutic agent within a nanoparticle the anticancer drug can be

protected from degradation before cell internalization or, alternatively, provide a more favorable uptake pathway for the cells via endocytosis followed by lysosomal degradation, which can potentially accelerate the conversion of Pt(IV) to its active form Pt(II). However, although the IC_{50} values for Zn-Pt(IV)-NCPs decreases with incubation time, slight differences between different cell lines were observed. As observed, the therapeutic action is also dependent on the cell type. Meanwhile for HeLa and BE(2)-M17 neuroblastoma cell lines the IC_{50} values obtained with cisplatin, Pt(IV) prodrug and Zn-Pt(IV)-NCPs are similar, in the case of MCF7 cells the toxicity is notably low in all cases.

To assess whether the differences in the cytotoxicity observed between the Zn-Pt(IV)-NCPs and the Pt(IV) prodrug can be attributed to the Zn metal ion present in the nanoparticles, a second generation of Pt-based NCPs incorporating Ni as metal node were synthesized and characterized. Characterization of these nanoparticles (Ni-Pt(IV)-NCPs,) revealed its analogous morphology and chemical composition in comparison with Zn-Pt(IV)-NCPs (See Supporting Information, Fig. S8-S10 and Table S2). The characterization by XRD revealed the amorphous nature of the nanoparticles (Fig. S11) and SEM analysis showed spherical shaped morphology with mean size of ~200 nm (Fig. S12). DLS measurements confirmed the stability of the nanoparticles under physiological conditions (PBS, 7.4 pH with 31 mg/ml BSA) having a hydrodynamic diameter close to 250 nm.

As observed in Table 2 the substitution of Zn by Ni in the nanoparticles does not affect the cytotoxicity, what discard the cytotoxic effect attributed to the metal node. As a control probe, $Zn(NO_3)_2 \cdot 6H_20$ and $Ni(NO_3)_2 \cdot 6H_20$ salt were tested and the results indicated low levels of citoxicity (Supporting Information, Table S3).

Table2. Comparative cytotoxicity of Ni-Pt(IV)-NCPs and Zn-Pt(IV)-NCPs.

	Ni-Pt(IV)-NCPs IC_{50} (μM)[1]		Zn-Pt(IV)-NCPs IC_{50} (μM)[1]	
Cell line	24 h	72 h	24 h	72 h
HeLa	302 ± 28	117 ± 24	218 ± 21	130 ± 27
MCF-7	339 ± 44	52 ± 6	249 ± 64	59 ± 8
BE(2)-M17	462 ± 46	81 ± 13	218 ± 21	133 ± 8

[1] Cell viability in the presence of the indicated compound and referred to Pt concentration.

458

459

460 3.5 Intracellular uptake and quantitation of DNA-bound Pt

461 Cellular uptake of the free Pt(IV) prodrug or nanostructured as NCPs was studied in HeLa,
462 BE(2)-M17 and MCF-7 cells, using ICP-MS as analytical technique to determine the amount of
463 platinum present in the intracellular medium. The cells were previously incubated in the
464 presence of 75 μM, of the Pt(IV) prodrug or Zn-Pt(IV)-NCPs, in terms of Pt concentration, for 5
465 h. Cisplatin was used as control using the same concentration based on amount of platinum and
466 under the same experimental conditions. As shown in Fig. 4, there was no statistically
467 significant difference concerning the amount of Pt detected inside the cells between the
468 prodrug-treated and nanoparticle-treated groups (P>0.05) for all of the cell lines studied.

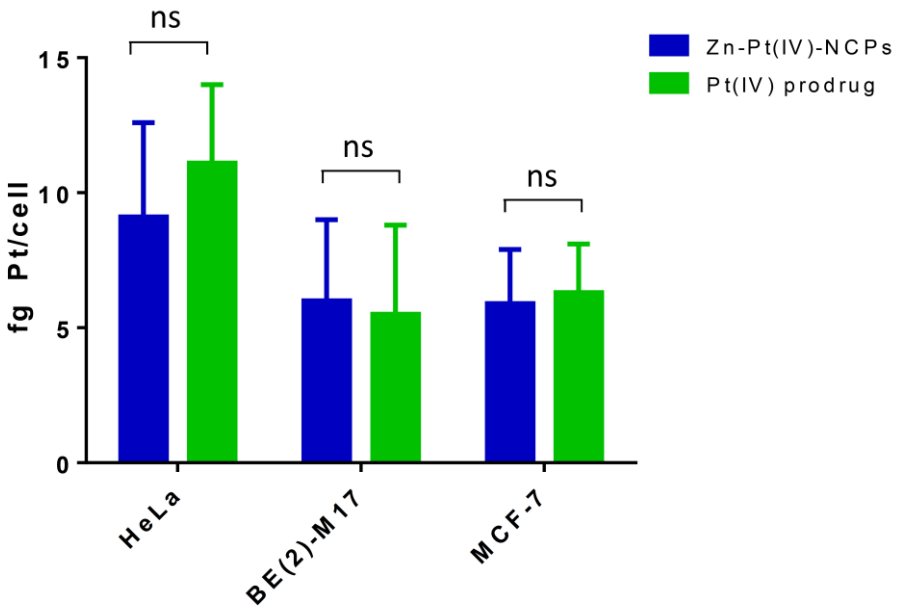

469

Fig. 4. Cellular uptake of Pt determined by ICP-MS. HeLa, BE(2)-M17 and MCF-7 cells were treated in the presence of Pt(IV) prodrug or Pt(IV)-NCPs at 75 μM for 6 h. After incubation, the total amount of internalized Pt was determined by ICP-MS. Data is shown as mean ± sd of three independent experiments performed in triplicate. An Unpaired t-test was performed to compare the Pt uptake between the three different agents: ns, not significative ($p > 0.05$).

These unexpected results do not correlate with the cytotoxicity effect if we attribute the cytotoxic effect to the amount of platinum. If fact it was expected a higher concentration of Pt inside the cells when the NCPs is used as previously observed with other kind of NCPs [21, 25]. In light of this, we performed additional uptake experiments to acquire a more precise quantification of the platinum that had not only reached the inner part of the cell, but also reached the nucleus and interacted with the nuclear double-stranded DNA (final target) in order to understand the higher cytotoxic effect associated to the nanostructured Pt(IV) prodrug in comparison to the free Pt(IV) prodrug.

In this second assay, the experimental conditions remains the same that the previous uptake study, but in this case the nuclear DNA of cells treated with cisplatin (control cells), Pt(IV) prodrug or Zn-Pt(IV)-NCPs was further purified and isolated. Then, the amount of Pt bound to the DNA was quantified by ICP-MS (see experimental section for more details). As shown in Fig. 5, results showed significantly higher concentrations of Pt bound to the DNA of cells treated with NCPs in comparison to those treated with the free Pt(IV) prodrug. As expected, the Pt concentrations in both cases were much lower compared to the treatment with the intrinsically active cisplatin.

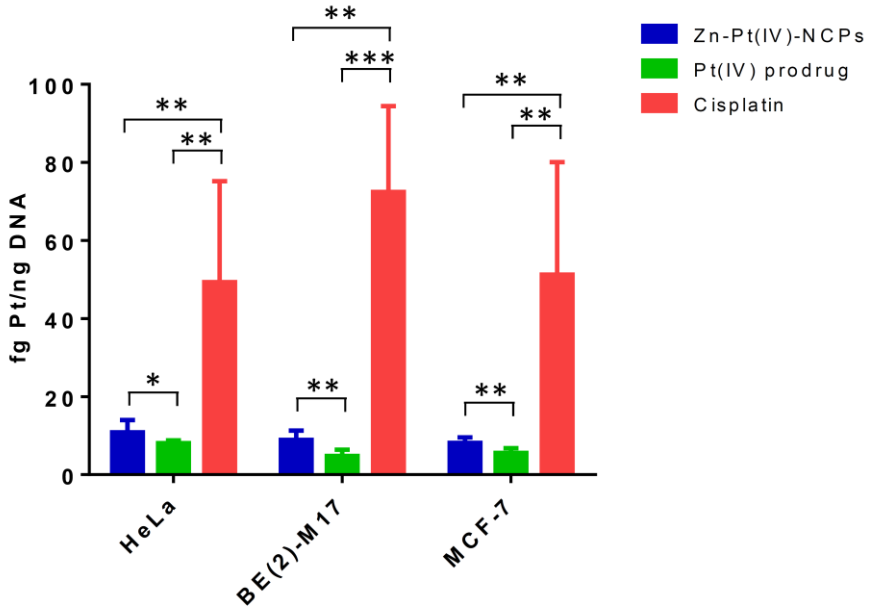

Fig. 5. Concentration of DNA-bound Pt determined by ICP-MS. HeLa, BE(2)-M17 and MCF-7 cells were treated in the presence of Pt(IV) prodrug or Zn-Pt(IV)-NCPs at 75 µM for 5 h. As control condition, cells were also treated with an equivalent Pt concentration of cisplatin. After treatment, the nuclear DNA was extracted from the cells, hydrolyzed with concentrated nitric acid and subjected to ICP-MS. Data is shown as mean ± Sd of three independent experiments performed in triplicate. An Unpaired t-test was performed to compare the DNA-bound Pt between the three different agents: * $p< 0.05$; ** $p< 0.01$; *** $p<0.0001$.

Therefore, these results bring light concerning the cytotoxic effect of the different formulations. These experimental data are in agreement with the observed cytotoxicity. Even that the amount of platinum internalized in cells was not achieving significant differences between the nanostructured and non-nanostructured Pt(IV) prodrug, platinum is actually more likely to reach the nuclei of cells when the prodrug is nanostructured, showing an enhancement in the cytotoxic effect upon nanostructuration. Shen and coworkers [29] investigated the kinetics and mechanism of reduction of Pt(IV) prodrug monomers and its derived Pt(IV)-coordinate polymers under different environments. These researchers showed that Pt(IV) in the polymers

was much easier reduced to Pt(II) in acidic conditions (such those found inside the cells in lysosomes/endosomes). Our results are, in line with this recent data, which suggest a different activation mechanism of the Pt(IV) prodrug upon the formation of the nanostructured coordination polymer. This hypothesis is consistent with DNA-binding experiments, in which we demonstrated that Zn-Pt(IV)-NCPs is indeed able to alter the mobility of plasmid DNA in the absence of reducing agent, while under the same conditions, the Pt(IV) prodrug monomer did not changed the migration of the plasmid DNA (Fig. 3). A number of previous studies demonstrated an enhanced effect of Pt(IV) prodrugs after its nanostructuration, however none of these works investigated the intracellular levels of Pt inside the cells, or neither the conversion of the prodrug.

Nanoparticles can often be engineered to have enhanced efficacy in the delivery of chemotherapeutic agents compared the parent drugs. One broad strategy in the nanodelivery of these drugs involves the study of cellular uptake, which usually correlates with the cytotoxic effect. In this report we show that the intracellular levels of Pt after treatment with a nanostructured Pt(IV) prodrug do not correlate with cytotoxicity, and highlight the importance of the study of other factors such the chemical interactions, activation mechanism and/or degradation of the nanostructured materials developed for specific platinum delivery.

4, Conclusions

In this study, we have successfully designed and synthetized nanostructured coordination polymer particles (NCPs) based on the polymerization of a Pt(IV) prodrug (DSCP), using Zn ions as metal nodes and bix as a coligand to induce the polymerization. The resulting nanoparticles (Zn-Pt(IV)-NCPs) are stable in physiologic conditions, and show an slow and sustainable release of the Pt(IV) prodrug during several hours. The cytotoxicity studies revealed

the enhanced antitumor activity of the nanoparticles respect to the free prodrug against the different cancer cell lines studied; HeLa, BE(2)-M17 and MCF-7. Although the enhanced efficacy demonstrated by the nanoparticles respect to the free prodrug, no increase in the total cellular uptake of Pt was observed. By contrast, the amount of Pt associated to the nuclear DNA of the cells treated with the nanoparticles was found to be higher than those cells treated with the free prodrug. The change of Zn by Ni in the NCPs formulation corroborated the non-existent toxicity related to the metal node. The obtaining results indicate that the nanostructuration have not a direct effect in the cellular uptake, but the polymerization of the Pt(IV) prodrug implies in some way a more facile conversion of the prodrug to the active cisplatinum molecule and the enhance of the cytotoxicity. The presented results have shown how the nanostructuration of a therapeutic agent or a prodrug can modify the bioavailability of the active specie and increase the therapeutic action based in different mechanism in comparison with non-structured molecules. In virtue of what was observed, many more efforts should be addressed to determine the different mechanisms of action of nanostructured materials and try to rationalize how the nanostructuration can modify the nature of the active specie.

Conflict of interest

The authors declare that they have no conflicts of interest with the contents of this article.

Acknowledgments

This work was supported by project MAT2012-38318-C03-02,MAT2015-70615-R, BIO2013-44973-R and BIO2016-78057-R from theSpanish Government and by FEDER–European Commission funds.ICN2 acknowledges support from the Severo Ochoa Programme of theSpanish Ministry of Economy, Industry and Competitiveness (MINECO,Grant SEV-2013-

559 0295). The ICN2 is funded by the CERCA programme/Generalitat de Catalunya. Authors
560 would also like to acknowledge thesupport of the TRANSAUTOPHAGY COST Action,
561 CA15138. NNAthanks the EU for a Marie Curie Intra-European Fellowship (FP6-MC-IEF-
562 629703).

563 References

564

565 [1] B. Rosenberg, L. VanCamp, J.E. Trosko, V.H. Mansour, Platinum compounds: a new class
566 of potent antitumour agents, Nature 222 (1969) 385-386.

567 [2] L.A. Zwelling, T. Anderson, K.W. Kohn, DNA-protein and DNA interstrand cross-linking
568 by cis- and trans-platinum(II) diamminedichloride in L1210 mouse leukemia cells and relation
569 to cytotoxicity, Cancer research 39 (1979) 365-369.

570 [3] S. Dasari, P.B. Tchounwou, Cisplatin in cancer therapy: molecular mechanisms of action,
571 European journal of pharmacology 740 (2014) 364-378.

572 [4] J.T. Hartmann, H.P. Lipp, Toxicity of platinum compounds, Expert opinion on
573 pharmacotherapy 4 (2003) 889-901.

574 [5] T. Karasawa, P.S. Steyger, An integrated view of cisplatin-induced nephrotoxicity and
575 ototoxicity, Toxicology letters 237 (2015) 219-227.

576 [6] A. Avan, T.J. Postma, C. Ceresa, A. Avan, G. Cavaletti, E. Giovannetti, G.J. Peters,
577 Platinum-induced neurotoxicity and preventive strategies: past, present, and future, The
578 oncologist 20 (2015) 411-432.

579 [7] L. Galluzzi, L. Senovilla, I. Vitale, J. Michels, I. Martins, O. Kepp, M. Castedo, G.
580 Kroemer, Molecular mechanisms of cisplatin resistance, Oncogene 31 (2012) 1869-1883.

581 [8] A.R. de Biasi, J. Villena-Vargas, P.S. Adusumilli, Cisplatin-induced antitumor
582 immunomodulation: a review of preclinical and clinical evidence, Clinical cancer research : an
583 official journal of the American Association for Cancer Research 20 (2014) 5384-5391.

584 [9] I. Ali, W.A. Wani, K. Saleem, A. Haque, Platinum compounds: a hope for future cancer
585 chemotherapy, Anti-cancer agents in medicinal chemistry 13 (2013) 296-306.

586 [10] S. Dilruba, G.V. Kalayda, Platinum-based drugs: past, present and future, Cancer
587 chemotherapy and pharmacology 77 (2016) 1103-1124.

588 [11] F. Meng, N. Han, Y. Yeo, Organic nanoparticle systems for spatiotemporal control of
589 multimodal chemotherapy, Expert opinion on drug delivery 14 (2017) 427-446.

590 [12] X. Duan, C. He, S.J. Kron, W. Lin, Nanoparticle formulations of cisplatin for cancer
591 therapy, Wiley interdisciplinary reviews. Nanomedicine and nanobiotechnology 8 (2016) 776-
592 791.

593 [13] C. He, D. Liu, W. Lin, Nanomedicine Applications of Hybrid Nanomaterials Built from
594 Metal-Ligand Coordination Bonds: Nanoscale Metal-Organic Frameworks and Nanoscale
595 Coordination Polymers, Chemical reviews 115 (2015) 11079-11108.

596 [14] T.C. Johnstone, K. Suntharalingam, S.J. Lippard, The Next Generation of Platinum Drugs:
597 Targeted Pt(II) Agents, Nanoparticle Delivery, and Pt(IV) Prodrugs, Chemical reviews 116
598 (2016) 3436-3486.

599 [15] N. Bertrand, J. Wu, X.Y. Xu, N. Kamaly, O.C. Farokhzad, Cancer nanotechnology: The
600 impact of passive and active targeting in the era of modern cancer biology, Adv Drug Deliver
601 Rev 66 (2014) 2-25.

602 [16] W.J. Rieter, K.M. Pott, K.M. Taylor, W. Lin, Nanoscale coordination polymers for
603 platinum-based anticancer drug delivery, Journal of the American Chemical Society 130 (2008)
604 11584-11585.

605 [17] L. Amorin-Ferre, F. Busque, J.L. Bourdelande, D. Ruiz-Molina, J. Hernando, F. Novio,
606 Encapsulation and release mechanisms in coordination polymer nanoparticles, Chemistry 19
607 (2013) 17508-17516.

608 [18] F. Novio, N. Simmchen, N. Vázquez-Mera, L. Amorín-Ferrer, D. Ruiz-Molina,
609 Coordination polymer nanoparticles in medicine, Coord. Chem. Rev. 257 (2013) 8.

610 [19] F. Novio, J. Lorenzo, F. Nador, K. Wnuk, D. Ruiz-Molina, Carboxyl group (-CO2 H)
611 functionalized coordination polymer nanoparticles as efficient platforms for drug delivery,
612 Chemistry 20 (2014) 15443-15450.

613 [20] R.C. Huxford-Phillips, S.R. Russell, D.M. Liu, W.B. Lin, Lipid-coated nanoscale
614 coordination polymers for targeted cisplatin delivery, Rsc Advances 3 (2013) 14438-14443.

615 [21] D.M. Liu, C. Poon, K.D. Lu, C.B. He, W.B. Lin, Self-assembled nanoscale coordination
616 polymers with trigger release properties for effective anticancer therapy, Nature
617 communications 5 (2014).

618 [22] N.N. Adarsh, F. Novio, D. Ruiz-Molina, Coordination polymers built from 1,4-
619 bis(imidazol-1-ylmethyl)benzene: from crystalline to amorphous, Dalton transactions 45 (2016)
620 11233-11255.

621 [23] F. Novio, J. Lorenzo, F. Nador, K. Wnuk, D. Ruiz-Molina, Carboxyl Group (-CO2H)
622 Functionalized Coordination Polymer Nanoparticles as Efficient Platforms for Drug Delivery,
623 Chem-Eur J 20 (2014) 15443-15450.

624 [24] I. Imaz, J. Hernando, D. Ruiz-Molina, D. Maspoch, Metal-organic spheres as functional
625 systems for guest encapsulation, Angewandte Chemie 48 (2009) 2325-2329.

626 [25] R.C. Huxford-Phillips, S.R. Russell, D. Liu, W. Lin, Lipid-coated nanoscale coordination
627 polymers for targeted cisplatin delivery, RSC advances 3 (2013) 14438-14443.

628 [26] D. Liu, C. Poon, K. Lu, C. He, W. Lin, Self-assembled nanoscale coordination polymers
629 with trigger release properties for effective anticancer therapy, Nature communications 5 (2014)
630 4182.

631 [27] Y. Shi, S.A. Liu, D.J. Kerwood, J. Goodisman, J.C. Dabrowiak, Pt(IV) complexes as
632 prodrugs for cisplatin, Journal of inorganic biochemistry 107 (2012) 6-14.

633 [28] J. Ruiz, J. Lorenzo, L. Sanglas, N. Cutillas, C. Vicente, M.D. Villa, F.X. Aviles, G. Lopez,
634 V. Moreno, J. Perez, D. Bautista, Palladium(II) and platinum(II) organometallic complexes with
635 the model nucleobase anions of thymine, uracil, and cytosine: antitumor activity and
636 interactions with DNA of the platinum compounds, Inorganic chemistry 45 (2006) 6347-6360.

637 [29] J. Yang, W. Liu, M. Sui, J. Tang, Y. Shen, Platinum (IV)-coordinate polymers as
638 intracellular reduction-responsive backbone-type conjugates for cancer drug delivery,
639 Biomaterials 32 (2011) 9136-9143.

640 [30] A. Binter, J. Goodisman, J.C. Dabrowiak, Formation of monofunctional cisplatin-DNA
641 adducts in carbonate buffer, Journal of inorganic biochemistry 100 (2006) 1219-1224.

642

643